6-1-2007

# The n-type Gd-doped $HfO_2$ to silicon heterojunction diode

Ihor Ketsman
*University of Nebraska - Lincoln*, iketsman@gmail.com

Yaroslav B. Losovyj
*University of Nebraska-Lincoln*, ylozovyy@indiana.edu

Andrei Sokolov
*University of Nebraska-Lincoln*, sokolov@unl.edu

J. Tang
*University of New Orleans, New Orleans, Louisiana*

Z. Wang
*University of New Orleans, New Orleans, Louisiana*

***See next page for additional authors***

Published in *Applied Physics A* **89** (2007), pp. 489–492; doi: 10.1007/s00339-007-4154-y


Submitted April 10, 2007; accepted May 23, 2007; published online June 28, 2007.

# The n-type Gd-doped $HfO_2$ to silicon heterojunction diode

I. Ketsman[1], Y. B. Losovyj[1,2], A. Sokolov[1], J. Tang[3], Z. Wang[3], K. D. Belashchenko[1], and P. A. Dowben[1,*]

[1] Department of Physics and Astronomy and the Nebraska Center for Materials and Nanoscience, University of Nebraska–Lincoln, P.O. Box 880111, Lincoln, NE 68588-0111, USA
[2] Center for Advanced Microstructures and Devices, Louisiana State University, 6980 Jefferson Highway, Baton Rouge, LA 70806, USA
[3] Department of Physics, University of New Orleans, New Orleans, Louisiana 70148, USA
* Corresponding author: fax 402-472-2879; email: pdowben@unl.edu

**Abstract**
Gd-doped $HfO_2$ films were deposited on p-type silicon substrates in a reducing atmosphere. Photoemission measurements indicate the n-type character of Gd-doped $HfO_2$ due to overcompensation with oxygen vacancies. The Gd 4*f* photoexcitation peak at 5.5 eV below the valence band maximum is identified using both resonant photoemission and first-principles calculations of the *f* hole. The rectifying (diode-like) properties of Gd-doped $HfO_2$ to silicon heterojunctions are demonstrated.

**PACS** 79.60.-i; 68.55.Ln; 29.40.Wk; 81.05.Je

---

While $HfO_2$ has attracted considerable attention as a high-$\kappa$ dielectric oxide [1–4], the gadolinium doping of a number of wide band gap semiconductors [5–9] suggests that Gd doping of $HfO_2$ may also lead to a dilute magnetic semiconductor [10, 11]. Moreover, semiconducting Gd-doped $HfO_2$ may provide a promising new class of materials for neutron detection technologies.

A gadolinium-based semiconductor diode might be better for neutron detection because of the large thermal neutron absorption cross section of gadolinium (on average ~ 46,000barns). The $^{157}Gd(n,\gamma)\rightarrow {}^{158}Gd$ and $^{155}Gd(n,\gamma)\rightarrow {}^{156}Gd$ reactions lead to the emission of low-energy gamma rays and conversion electrons, most of which are emitted at energies below 220 eV [12–15]. The appeal of using $^{157}Gd$ is due to its large thermal neutron cross section of 240 000 barns [16, 17]. Although sensitive to gamma radiation, the big advantage of gadolinium over boron is not only the high neutron capture cross section but also that this cross section extends to higher neutron energies (200 meV)thanis the case for boron. While all-boron-carbide neutron detectors have been demonstrated [18–20], and their potential detection efficiency is much higher than that of many semiconductor materials (likely well above 50% for $^{10}B$-enriched devices), the drawback to all boron-based devices is the need for a moderator to reduce the neutron kinetic energies to 25–30 meV. Fissile radiation sources like $^{235}U$ or $^{239}Pu$ produce 1–2MeV neutrons, so the moderator must be significant.

Since neutron capture by gadolinium leads to production of a conversion electron, the pulse height will be smaller than in the case of neutron capture by boron ($10^4$ charges versus $10^6$ per neutron capture). Accordingly, it is advantageous to see if a Gd-doped $HfO_2$ diode can be fabricated that can be impedance matched and compatible with a high gain, low noise amplifier. A heterojunction diode with silicon would serve this purpose. Although Gd is expected to be a p-type dopant in $HfO_2$, we attempted to fabricate a heterojunction diode of n-type Gd-doped $HfO_2$ with silicon by overcompensating the Gd acceptor states by donor states introduced by oxygen vacancies, as such a device would likely have a larger depletion region and therefore larger detection volume.

The Gd-doped (3 at. %) $HfO_2$ films were deposited on single crystal silicon (100) p-type substrates using pulsed laser deposition (PLD) at a growth rate of about 0.15 Å/s. A Gd–$HfO_2$ target was prepared by standard ceramic techniques using $HfO_2$ and $Gd_2O_3$ powders, as described elsewhere [11]. Before the deposition, the Si(100) substrates were cleaned with diluted HF acid, rinsed with acetone, and were then immediately put in the vacuum chamber. Before deposition, the surface of the Si wafers was sputter cleaned in a plasma of $H_2$ (8%) and Ar (92%) mixture created by a DC sputtering gun operating in the reverse bias mode.The films were deposited at a substrate temperature of 500 °C. The chamber was pumped to a base pressure of $3 \times 10^{-7}$ Torr and the deposition was carried out in a mixture of $H_2$ and Ar (8% $H_2$) to introduce the necessary oxygen vacancies. The vacuum was maintained at $10^{-5}$ Torr during the deposition. The doping level was determined from the target composition, with companion measurements using near edge X-ray adsorption spectroscopy (NEXAFS), and on separate samples by X-ray emission spectroscopy or energy dispersive analysis of X-rays (XES or EDAX) for similarly prepared samples. The complementary spectroscopies show that the films and the target have essentially the same composition.

X-ray diffraction (XRD) patterns show that the resulting approximately 250-nm-thick $HfO_2$ films are in a single monoclinic phase with strong texture growth, with about 3% strain compared with the undoped $HfO_2$ (Figure 1). From the largest peak near 28 degrees ($2\theta$), it is estimated that the lattice spacing for (–1,1,1) is increased by $d = 0.0030$ nm, from 0.3147(1) nm for the undoped $HfO_2$ films to 0.3177(1) nm for Gd-doped samples (Figure 1). The peak is shifted to lower angles by 0.338 degrees.

As just noted, the films were deposited in 8% $H_2$–Ar flow, in an attempt to create more oxygen vacancies. To determine the placement of the Fermi level, angle-resolved photoemission experiments were performed using the 3m toroidal grating monochromator (3m TGM) beam line in a UHV chamber previously described [21, 22]. The Fermi level ($E_F$) was established from a gold film in electrical contact with the sample and measurements were carried out at ambient temperatures.

From Figure 2, it is clear that the valence band edge is placed well away from the Fermi level for both Gd-doped and undoped $HfO_2$ films. The Hf 4*f* binding energies, at 18–21 eV binding energy, are substantially larger than those reported by Renault and coworkers [23], and Hf 4*f* binding energies and the valence band edge are slightly larger than those reported elsewhere [24–26]. Indeed, with Gd doping, the Hf 4*f* binding energies increase, as seen in Figure 2. These photoemission results indicate that the Gd-doped $HfO_2$ may have n-type character (i.e. the Fermi level is closer to the conduction band edge than to the valence band edge).

The increase with Gd doping in the intensity of the photoemission features in the oxygen 2*p* region of the valence band, at 5 to 10 eV binding energy, relative to the Hf 4*f* features at 18–21 eV binding energies, suggests that there are Gd 5*d* contributions to the these lower binding energy features, as is expected from studies of $HfO_2$–$Y_2O_3$ composite films [27]. In Figure 2, one can clearly see a shoulder on the broad photoemission peak at the binding energy of 9–10 eV. In order to assist in the identification of this feature, we performed resonant photoemission (i.e. constant initial state spectroscopy) measurements; the results are shown in Figure 3. The photoelectron intensity, determined from the feature at about 9.5eV binding energy (from the Fermi level), is strongly enhanced at about 148 eV photon energy. This resonant enhancement has been plotted for various photon energies, as shown in the inset to Figure 3. It is clear that the resonant enhancements in the photoemission intensity, from this 9.5eV binding energy final state, occur at photon energies corresponding to the binding energy of the Gd $4d_{3/2}$ (147 eV) shallow core. Thus, this feature at 9.5eV binding energy has strong Gd weight, and the resonant photoemission process occurs because of an excitation from the 4*d* cores to a bound state, but with a final state identical to that resulting from direct photoemission from Gd 4*f* states [28–30], that is to say is due to constructive interference between the direct 5*f* photoionization and a $4d^{10}4f^7 \rightarrow 4d^9 4f^8 \rightarrow 4d^{10}4f^6 + e^-$ super Coster–Kronig transition [29], leading to a classic Fano resonance.

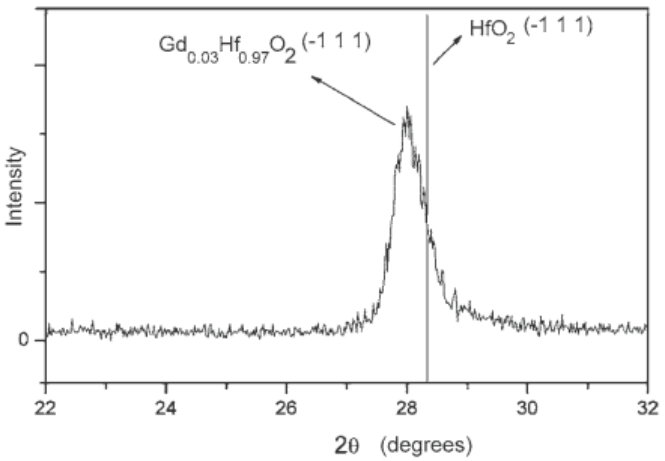


**Figure 1** Part of the XRD pattern of the film is shown in the figure. Besides Si peaks, the XRD is consistent with that of $HfO_2$ in a simple monoclinic structure. From the largest peak near 28 degrees ($2\theta$), shown here, we estimated that the lattice spacing for (–1,1,1) is increased by $d$ = 0.0030(1) nm. The peak is shifted to lower angles by 0.338 degrees.

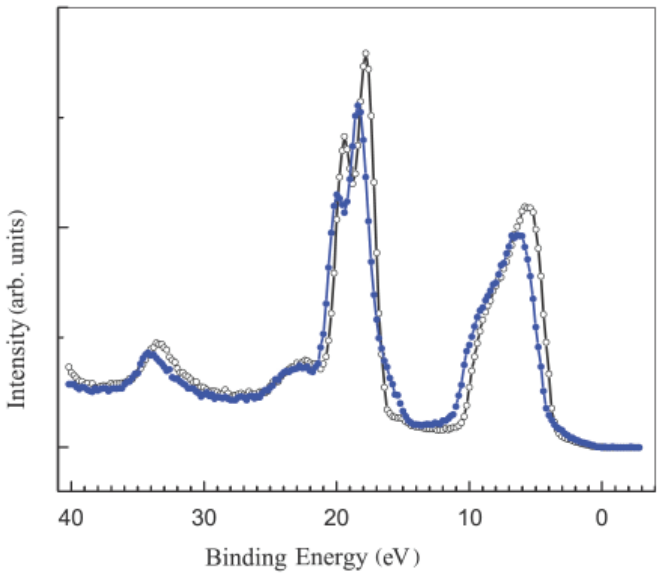


**Figure 2** Different band intensities for pristine (*open dots*) and Gd-doped films of $HfO_2$ (*filled blue dots*). The photon energy is 100 eV and the light incidence angle is 45°. All photoelectrons were collected along the surface normal at $T$ = 320 °C.

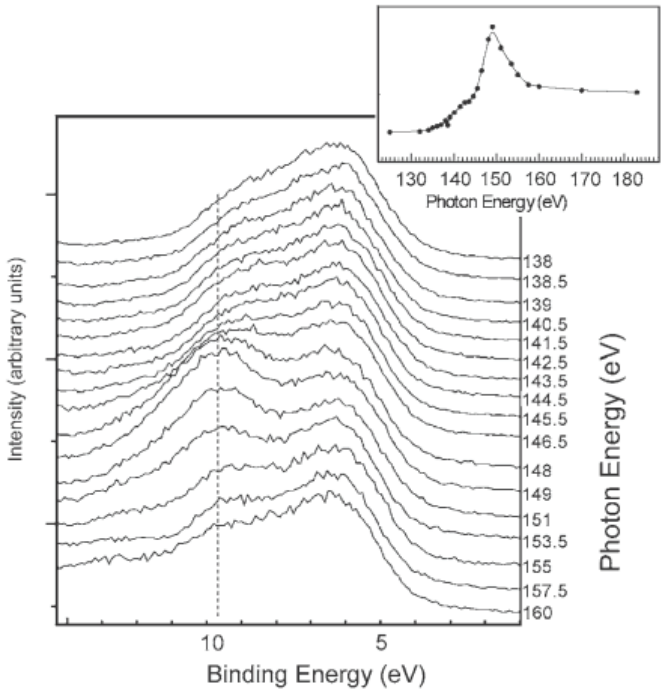


**Figure 3** Resonant photoemission for Gd-doped films of $HfO_2$. The light incidence angle is 45°. All photoelectrons were collected along the surface normal

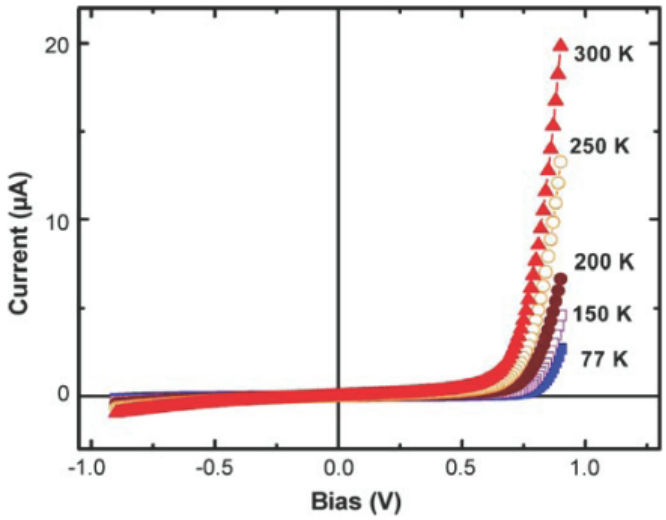


**Figure 4** A heterojunction diode constructed from Gd-doped $HfO_2$ on p-type silicon, as a function of temperature

In order to further verify the character associated with observed photoemission features, we performed first-principles electronic structure calculations using the full-potential linear augmented plane-wave (FLAPW) method in the local density approximation (LDA). To simulate the photoemission process from the 4 *f* shell, we consider a supercell containing one Gd impurity atom. We include the 4 *f* electrons on both Hf and Gd atoms in the core (which by itself is an excellent approximation) and calculate the LDA total energies of the supercell with the 4 *f* occupation on the Gd atom fixed at seven for the ground state and six for the photoexcited 4 *f* hole. (The 4 *f* core on the Gd atom is fully spin polarized.) The difference between these energies is the 4 *f* binding energy referenced from the valence band maximum. The accuracy of this method is typically better than 1eV [31].

Instead of the complicated monoclinic phase, the calculations for the Gd impurity were performed for the high-temperature fluorite phase. This is justified because on a crude level the electronic properties of the two phases are qualitatively similar. In particular, the calculated band gaps (3.8eV for the fluorite and 4.0eV for the monoclinic phase, the experimental value being 5.7eV [26, 32]) and valence band widths (6.5eV for the fluorite and 5.6eV for the monoclinic phase) are quite similar.

The Hf atoms occupy an fcc sublattice in the fluorite phase. A simple cubic supercell was chosen containing four Hf and eight O sites, and one of the four Hf atoms was replaced by Gd. Although there is nominally a very large size mismatch between Hf and Gd, our calculations show that Gd is readily accommodated in the fluorite $HfO_2$ with a rather small distortion of the surrounding lattice. These results are consistent with experimental observations showing that rare-earth substitution tends to stabilize the fluorite phase in $HfO_2$ with respect to the monoclinic one [33, 34]. Our calculations show that Gd is a p-type dopant introducing very shallow acceptor states, consistent with expectations.

From the 4 *f* -hole calculations, we obtained the Gd 4 *f* binding energy of about 5.5eV below the valence band maximum, which is in excellent agreement with the photoemission data shown in Figures 2 and 3. This binding energy is smaller compared to the Gd metal (8.6eV) because of the electrostatic upshift resulting from the charge transfer to O. This upshift also raises the Gd 5*d* states into the conduction band compared to the Gd metal where they straddle the Fermi level. The binding energy reduction due to the electrostatic upshift is partially offset by less effective screening of the 4 *f* hole in the insulator compared to metallic Gd. Using the 4 *f* -hole method for a pure fluorite $HfO_2$ supercell of the same size, we also found the Hf 4 $f_{7/2}$ binding energy of 14.5eV referenced from the valence band maximum (we took into account that the photoexcited electron goes into an n-type level about 0.5eV below the conduction band minimum). The 4 $f_{7/2}$ is the lower-binding-energy component of the Hf 4 *f* doublet, so that this value corresponds to the upper (stronger) subpeak in Figure 2. Similar to Gd peak, the agreement with experiment is excellent.

We fabricated several diodes to illustrate the n-type band offset of the Gd-doped $HfO_2$ relative to p-type silicon. The heterojunction of Gd-doped $HfO_2$ and p-type silicon forms an excellent diode, as shown in Figure 4. While these data do not conclusively show the dominant carrier, they suggest that oxygen vacancies can overcompensate the Gd acceptor states without completely destroying the semiconductor properties, consistent with the photoemission.

The present results indicate that a p–n heterojunction diode can be formed with strongly textured monoclinic Gd-doped $HfO_2$ on Si(100). This result is very promising for a number of applications, but we expect that the fluorite phase of Gd-doped $HfO_2$ may be a superior semiconductor. The fluorite phase should be stabilized by increased Gd doping [33, 34], with the added benefit that adding Gd will also increase the neutron opacity of the device, for smaller collection volumes.

**Acknowledgements**

The authors acknowledge insightful discussions with David Wisbey, Andre Petukhov, and J. Brand. This work was supported by the Office of Naval Research (Grant No. N00014-06-10616), the Defense Threat Reduction Agency (Grant No. HDTRA1-07-10008), and the Nebraska Research Initiative.

**References**

1 M. McCoy, Chem. Eng. News **83**, 26 (2005)

2 B.H. Lee, L. Kang, W.-J. Qi, R. Nieh, K. Onishi, J.C. Lee, Tech. Dig. Int. Electron. Dev. Meet. **1999**, 133 (1999)

3 M. Gutowski, J.E. Jaffe, C.-L. Liu, M. Stoker, R.I. Hegde, R.S. Raj, P.J. Tobin, Appl. Phys. Lett. **80**, 1897 (2002)

4 K.P. Bastos, J. Morais, L. Miotti, R.P. Pezzi, G.V. Soares, I.J.R. Baumvol, R.I. Hegde, H.H. Tseng, P.J. Tobin, Appl. Phys. Lett. **81**, 1669 (2002)

5 S. Dhar, O. Brandt, M. Ramsteiner, V.F. Sapega, K.H. Ploog, Phys. Rev. Lett. **94**, 037 205 (2005)

6 S. Dhar, L. Pérez, O. Brandt, A. Trampert, K.H. Ploog, J. Keller, B. Beschoten, Phys. Rev. B **72**, 245 203 (2005)

7 S. Dhar, T. Kammermeir, A. Ney, L. Pérez , K.H. Ploog, A. Melnikov, A.D. Wieck, Appl. Phys. Lett. **89**, 062 503 (2006)

8 L. Pérez, G.S. Lau, S. Dhar, O. Brandt, K.H. Ploog, Phys. Rev. B **74**, 195 207 (2006)

9 K. Potzger, S.-Q. Zhou, F. Eichhorn, M. Helm, W. Skorupa, A. Mücklich, J. Fassbender, T. Herrmannsdorfer, A. Bianchi, J. Appl. Phys. **99**, 063 906 (2006)

10 M. Venkatesan, C.B. Fitzgerald, J.D.M. Coey, Nature **430**, 630 (2004)

11 W. Wang, Y. Hong, M. Yu, B. Rout, G.A. Glass, J. Tang, J. Appl. Phys. **99**, 08M117 (2006)

12 K.S. Shah, L. Cirignano, R. Grazioso, M. Klugerman, P.R. Bennet, T.K. Gupta, W.W. Moses, M.J. Weber, S.E. Derenzo, (2001) http://breast.lbl.gov/~wwwinstr/publications/Papers/LBNL-50253.pdf

13 S.F. Mughabghab, *Neutron Cross Sections*, vol. 1 (Academic Press, New York, 1981)

14 P.L. Reeder, Nucl. Instrum. Methods Phys. Res. A **353**, 134 (1994)

15 B. Gebauer, C. Schulz, T. Wilpert, Nucl. Instrum. Methods Phys. Res. A **392**, 68 (1997)

16 A. Mireshghi, G. Cho, J.S. Drewery, W.S. Hong, T. Jing, H. Lee, S.N. Kaplan, V. Perez-Mendez, IEEE Trans. Nucl. Sci. **41**, 915 (1994)

17 D.I. Garber, R.R. Kinsey, *BNL 325: Neutron Cross Sections*,vol. 2, 3rd edn. (Brookhaven National Laboratory, Upton, 1976)

18 A.N. Caruso, R.B. Billa, S. Balaz, J.I. Brand, P.A. Dowben, J. Phys. C Condens. Matter **16**, L139 (2004)

19 A.N. Caruso, P.A. Dowben, S. Balkir, N. Schemm, K. Osberg, R.W. Fairchild, O.B. Flores, S. Balaz, A.D. Harken, B.W. Robertson, J.I. Brand, Mater. Sci. Eng. B **135**, 129 (2006)

20 K. Osberg, N. Schemm, S. Balkir, J.I. Brand, S. Hallbeck, P. Dowben, IEEE Sens. J. **6**, 1531 (2006)

21 T. Komesu, H.-K. Jeong, J. Choi, C.N. Borca, P.A. Dowben, A.G. Petukhov, B.D. Schultz, C.J. Palmstrøm, Phys. Rev. B **67**, 035 104 (2003)

22 C.-G. Duan, T. Komesu, H.-K. Jeong, C.N. Borca, W.-G. Yin, J. Liu, W.N. Mei, P.A. Dowben, A.G. Petukhov, B.D. Schultz, C.J. Palmstrøm, Surf. Rev. Lett. **11**, 531 (2004)

23 O. Renault, D. Samour, J.-F. Damlencourt, D. Blin, F. Martin, S. Mathon, N.T. Barrett, P. Besson, Appl. Phys. Lett. **81**, 3627 (2002)

24 S. Suzer, S. Sayan, M.M. Banaszak Holl, E. Garfunkel, Z. Hussain, N.M. Hamdan, J. Vac. Sci. Technol. A **21**, 106 (2003)

25 S. Sayan, T. Emge, E. Garfunkel, X. Zhao, L. Wielunski, R.A. Bartynski, D. Vanderbilt, J.S. Suehle, S. Suzer, M.M. Banaszak Holl, J. Appl. Phys. **96**, 7485 (2004)

26 S. Sayan, R.A. Bartynski, X. Zhao, E.P. Gusev, D. Vanderbilt, M. Croft, M.M. Banaszak Holl, S. Suzer, Phys. Stat. Solidi B **241**, 2246 (2004)

27 M. Komatsu, R. Yasuhara, H. Takahashi, S. Toyoda, H. Kumigashira, M. Oshima, D. Kukuruznyak, T. Chikyow, Appl. Phys. Lett. **89**, 172 107 (2006)

28 P.A. Dowben, D. Li, J. Zhang, M. Onellion, J. Vac. Sci. Technol. A **13**, 1549 (1995)

29 T. Kachel, R. Rochow, W. Gudat, R. Jungblut, O. Rader, C. Cabone, Phys. Rev. B **45**, 7276 (1992)

30 R.F. Sabirianov, W.N. Mei, J. Lu, Y. Gao, X.C. Zeng, R.D. Bolskar, P. Jeppson, N. Wu, A.N. Caruso, P.A. Dowben, J. Phys. C Condens. Matter **19**, 082 201 (2007)

31 A.J. Freeman, B.I. Min, M.R. Norman, in *Handbook on the Physics and Chemistry of Rare Earths*, vol. 10, ed. by K.A. Gschneider, L. Eyring, S. Hüfner (Elsevier, Amsterdam, 1987), p. 165

32 T.V. Perevalov, V.A. Gritsenko, S.B. Erenburg, A.M. Badalyan, H. Wong, C.W. Kim, J. Appl. Phys. **101**, 053 704 (2007)

33 J. Wang, H.P. Li, R. Stevens, J. Mater. Sci. **27**, 5397 (1992)

34 E. Rauwel, C. Dubourdieu, B. Holländer, N. Rochat, F. Ducroquet, M.D. Russell, G. van Tendeloo, B. Pelissier, Appl. Phys. Lett. **89**, 012 902 (2006)